REPUBLIC OF AZERBAIJAN

On the rights of the manuscript

ABSTRACT

of the dissertation for the degree of Doctor of Philosophy

INVESTIGATION OF THE EFFECT OF STABILIZERS, TEMPERATURE AND DOPING PROCESSES WITH Cu, Ag ON THE PROPERTIES OF Co_3O_4 AND NiO NANOPARTICLES

Speciality: 2317.01 – Nanochemistry and nanomaterials

Field of science: Chemistry

Applicant: **Sevinj Jalal Mammadyarova**

Baku – 2025

The work was performedat the Scientific Laboratory of Nanoresearch of Baku State University.

Supervisors:
academician of ANAS, doctor of chemical sciences, professor
Abel Mammadali Maharramov
PhD in physics and mathematics, associate professor
Mustafa Bayram Muradov

Official opponents:
academician of ANAS, doctor of chemical sciences, professor
Vagif Maharram Abbasov,
academician of ANAS, doctor of chemical sciences, professor
Adil Abdulkhalig Garibov,
corresponding member of ANAS, doctor of chemical sciences, professor
Islam Israfil Mustafayev

Dissertation Council BED 2.16 of Supreme Attestation Comission under the President of the Republic of Azerbaijan operating at Baku State University

Chairman of the Dissertation council:
doctor of chemical sciences, professor
Ibrahim Garib Mammadov

Scientific secretary of the Dissertation council:
doctor of chemical sciences, associate professor
Farid Nadir Naghiyev

Chairman of the scientific seminar:
academician of ANAS, doctor of chemical sciences, professor
Vagif Majid Farzaliyev

ELMİ KATİB
SCIENTIFIC SECRETARY
"18" 04 2025

GENERAL CHARACTERISTICS OF THE WORK

Relevance of the topic and the degree of development. The properties of nanosized materials differ dramatically compared to their bulk counterparts. It increases the potential application areas of these materials. It is possible to control the size, structure, and shape of nanoscale particles and enhance their physicochemical properties by applying various physical and chemical methods. Among transition metal oxides, cobalt oxide and nickel oxide nanoparticles have attracted great attention and potential applications due to their unique optical, catalytic, electrical, and magnetic properties. Cobalt oxide and nickel oxide nanostructures are known to have a wide range of applications, such as catalysts, gas sensors, supercapacitors, electrochemical sensors, electrochromic devices, dye-sensitized photocathodes, anode materials in Li-ion batteries, and elements of photovoltaic, optoelectronic, and magnetic devices. Recently, the doping of metal oxide nanoparticles with various elements (transition metals, noble metals, non-metals, rare earth elements, and metal oxides) has been widely applied. It is possible to enhance the physical-chemical properties of nanoparticles by the doping process.

The object and subject of the research. The objects of research are Co_3O_4 thin films synthesized by the SILAR method on two different substrates (glass and silicon), Co_3O_4 nanoparticles synthesized by the sonochemical method in the presence of various stabilizing agents, and Co_3O_4 and NiO nanoparticles doped with Cu, Ag synthesized by this method. The study of the effect of stabilizing agents, temperature, and doping processes with Cu, Ag on the structural and optical properties of the synthesized Co_3O_4 and NiO nanoparticles is the main subject of the research.

The aims and tasks of the research. The main ***goal*** of the dissertation work is to synthesize Co_3O_4 and NiO nanoparticles (NPs) using various methods, to study their structure, optical and dielectric properties, surface morphology and chemical composition, and to investigate the effects of stabilizers, temperature, and doping processes with different concentrations of Cu and Ag on the mentioned properties of these NPs.

To achieve the set goal, the following ***tasks*** were performed:

- Synthesis of Co_3O_4 thin films by SILAR method on various substrates;
- Synthesis of Co_3O_4 NPs using different stabilizers [polyvinyl alcohol (PVA), 3-mercaptopropionic acid (3-MPA) and styrene] and studying the effect of these stabilizers on the properties of the formed NPs;
- Investigation of various doping methods and study of the effect of the doping process on the properties of NPs;
- Synthesis of $Cu_xCo_{3-x}O_4$, $Ag_xCo_{3-x}O_4$, $Cu_xNi_{1-x}O$ and $Ag_xNi_{1-x}O$ (x=0.02, 0.04, 0.06, 0.1) nanoparticles by sonochemical method and study of the effect of the doping process on the properties of the formed NPs;
- Synthesis of Ni/NiO nanochains by oxidation-reduction method and study of the effect of thermal treatment at different temperatures on the structural and optical properties of the obtained nanostructures.

Research methods. The structural properties of the samples were analyzed by X-ray diffraction (XRD), optical properties were measured by Ultraviolet-visible spectroscopy (UV-Vis.) (in the wavelength range of 190-1100 nm) and Infrared spectroscopy (IR) (in the wavenumber range of 400-4000 cm^{-1}), the morphological properties and size were studied using scanning electron microscopy (SEM) and transmission electron microscopy (TEM), the elemental composition was studied using energy-dispersive X-ray spectroscopy (EDS).

Basic provisions for defense:

1. Synthesis of Co_3O_4 nanoparticles by the SILAR method on different substrates and the effect of the nature of the substrates on the structure of the formed nanoparticles;
2. Effect of various stabilizing agents on the size and optical properties of Co_3O_4 nanoparticles obtained by the sonochemical method;
3. Effect of doping process with different concentrations of Cu and Ag on the structure, optical and photocatalytic properties of Co_3O_4 nanoparticles synthesized by the sonochemical method;

4. Effect of doping process with different concentrations of Cu and Ag on the structure, optical and photocatalytic properties of NiO nanoparticles synthesized by the sonochemical method;
5. The effect of different temperatures on the structure and optical properties of Ni/NiO nanochains synthesized by the oxidation-reduction method

The scientific novelty of the research.

1. By using different stabilizing agents and varying the concentration of copper and silver as dopants, it has been possible to control the structure, size, chemical composition, morphology, as well as the optical and photocatalytic properties of Co_3O_4 and NiO nanoparticles synthesized via the sonochemical method.
2. No peaks belonging to the dopants were observed in the X-ray diffractograms of Co_3O_4 and NiO nanoparticles at a concentration of dopants up to 10%. This indicates the successful incorporation of the dopants into the Co_3O_4 and NiO lattice.
3. Among cobalt oxide NPs doped with different concentrations of Cu and Ag, an increase in photodegradation efficiency was observed in the presence of the $Cu_{0.02}Co_{2.98}O_4$ compound compared to undoped NPs.
4. It was possible to control the optical properties of Ni/NiO nanochains synthesized by the oxidation-reduction method at temperatures of 400°C, 500°C, 600°C.

Theoretical and practical significance of research. The synthesized nanoparticles, having a wide band gap, can be considered as a promising material for sensors and solar cells. The possibility of using doped nanostructures as photocatalysts for the degradation of methylene blue dye under visible light was investigated, and an increase in the results was observed compared to undoped nanostructures.

Approbation and application. 21 scientific works (11 articles and 10 theses) on the topic of the dissertation have been published in local and foreign journals. Five articles were published in journals indexed in the Web of Science Clarivate Analytics and Scopus databases. The results obtained were reported at several scientific conferences at the republican and international levels:

–II International scientific conference of young researchers (Baku, 27-28 April 2018);
–5th International Conference “Nanotechnologies” NANO-2018 (Tbilisi, 19-22 November 2018);
–1st International science and engineering conference (Baku, 29-30 November 2018);
– 2nd International Conference on Light and Light-Based Technologies (Ankara, 26-28 May 2021);
–1st International Symposium on Recent Advances in Fundamental and Applied Sciences (ISFAS-2021) (Erzurum, 10-12 September 2021);
–6th International Conference “Nanotechnology” (GTUnano20) (Tbilisi, 4-7 October 2021);
–7th International Conference MTP-2021: Modern Trends in Physics (Baku, 15-17 December 2021);
–Cukurova 8th International Scientific Researches Conference (Adana, 15 - 17 April 2022);
–Nanoscience & Nanotechnology Conference (Laboratori Nazionali di Frascati (Rome, 29 May-1 June 2023);
–8th International Conference: "MTP-2023" Modern Trends Physics (Baku, 30 November - 1 December 2023).

The name of the institution where the dissertation work was performed. The dissertation work was carried out in the Scientific Laboratory of Nano Research at Baku State University.

The total volume of the dissertation with a symbol indicating the volume of the structural sections of the dissertation separately. The dissertation consists of 196 pages (174812 characters), introduction (8691 characters), 3 chapters (first chapter-52102 characters, second chapter-25591 characters, third chapter-85840 characters), results (2588 characters), a list of 203 references, a list of abbreviations and symbols. The dissertation also includes 98 figures and 16 tables.

Personal contribution of the author. The author personally participated in reviewing the literature on the topic of the dissertation, conducting experiments, analyzing and explaining the results of the analysis of the obtained products using various research methods, preparing articles and theses, as well as submitting them to journals for publication.

CONTENT OF THE DISSERTATION WORK

The relevance of the topic is justified, the purpose of the work, the tasks performed to achieve the set goal, the object and subject of the research, research methods, the scientific novelty of the work, the main scientific provisions presented for defense are indicated, the practical and theoretical importance of the work is justified, the approbation of the results, information about the structure and volume of the dissertation work has been explained **in the introduction**.

In the first chapter, a literature review was prepared by examining the synthesis of cobalt oxide and nickel oxide NPs by various methods, their physical-chemical properties, application areas, and prospectiveness.

The second chapter reflects experimental work on the synthesis of cobalt oxide and nickel oxide NPs by various methods (SILAR and sonochemical). The synthesis of cobalt oxide thin films using the SILAR method was carried out at room temperature on two different substrates (glass and silicon) with varying cycles and different concentrations of the oxidizing agent (H_2O_2). The synthesis of cobalt oxide NPs by the sonochemical method was carried out in the presence of various stabilizers. In addition, during the synthesis using this method, cobalt oxide and nickel oxide NPs were doped with Ag and Cu. Ni/NiO nanochains were synthesized by the oxidation-reduction method under the influence of different magnetic field intensities, and their structure and optical properties were investigated depending on the oxidation temperature.

In the third chapter, the structure and properties of the samples were studied. Figures 1 and 2 show the X-ray diffractograms before and after thermal treatment of the films synthesized using 1% and 3% H_2O_2 on a glass substrate at different deposition cycles. In the X-ray diffractogram of the samples before thermal treatment, the peak corresponding to the plane with (003) Miller indice at 20º value of 2θ corresponds to polycrystalline cobalt oxyhydroxide [CoO(OH)] (JCPDS-14-0673). The broad peak observed in the diffractogram corresponds to the amorphous glass substrate. After thermal treatment of the samples at 300°C for 3 hours, no peak corresponding to cobalt oxide was observed. This indicates that the synthesized thin films had an amorphous structure.

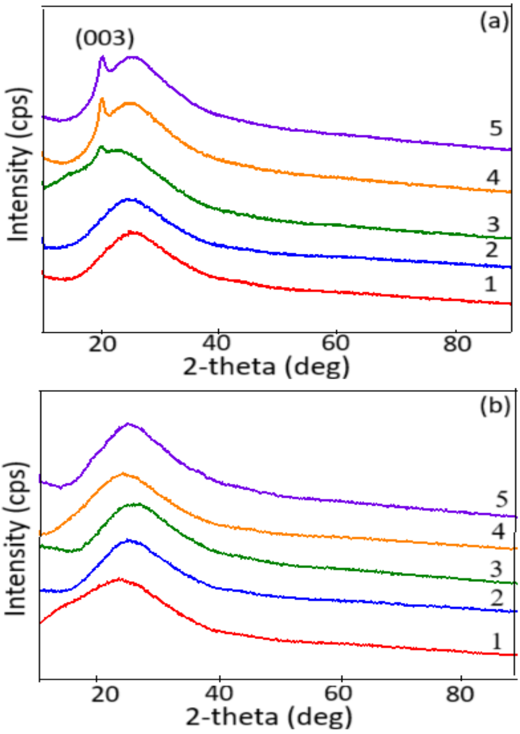

Figure 1. XRD analysis of (a) CoO(OH) and (b) Co_3O_4 films synthesized using 1% H_2O_2 on a glass substrate; 1- 40 cycles; 2 – 60 cycles; 3 – 80 cycles; 4-100; 5 – 120 cycles.

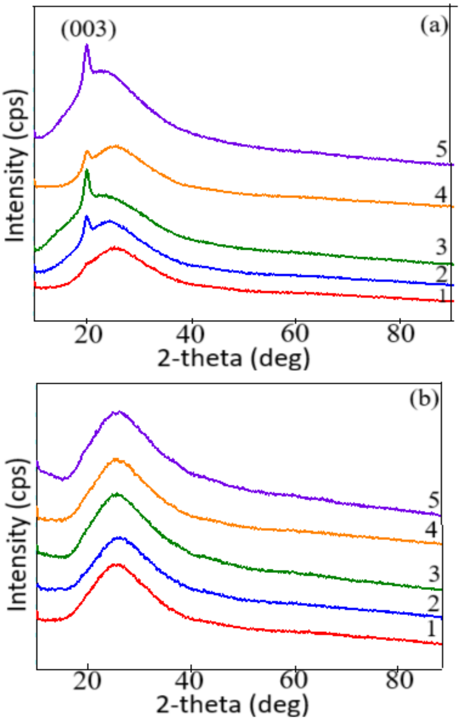

Figure 2. XRD analysis of (a) CoO(OH) and (b) Co_3O_4 films synthesized using 3% H_2O_2 on a glass substrate; 1- 40 cycles; 2 – 60 cycles; 3 – 80 cycles; 4-100; 5 – 120 cycles.

Figure 3 shows the X-ray diffractograms of films deposited on a silicon substrate for 60 cycles before and after thermal treatment. The peaks observed at $2\theta=14.37^\circ$, 17.17°, 28.44° in the diffractogram of the films synthesized using 3% H_2O_2 on the silicon substrate before thermal treatment correspond to the silicon substrate. In addition, similar to the RD analysis results of the films synthesized on the glass substrate, the peak corresponding to CoO(OH) was observed at $2\theta=20.02^\circ$ (in the films synthesized using 3% H_2O_2) and $2\theta=20.22^\circ$ diffraction angles (in the films synthesized using 1% H_2O_2). After thermal treatment of the synthesized films using 1% and 3% H_2O_2 on a silicon substrate at 300ºC, small intensity peaks were observed in the diffractogram at $2\theta=19.26^\circ$, 36.98° and $2\theta=39.54^\circ$, 59.16° respectively.

These results indicate the formation of poorly crystalline Co_3O_4 (JCPDS-00-009-0418).

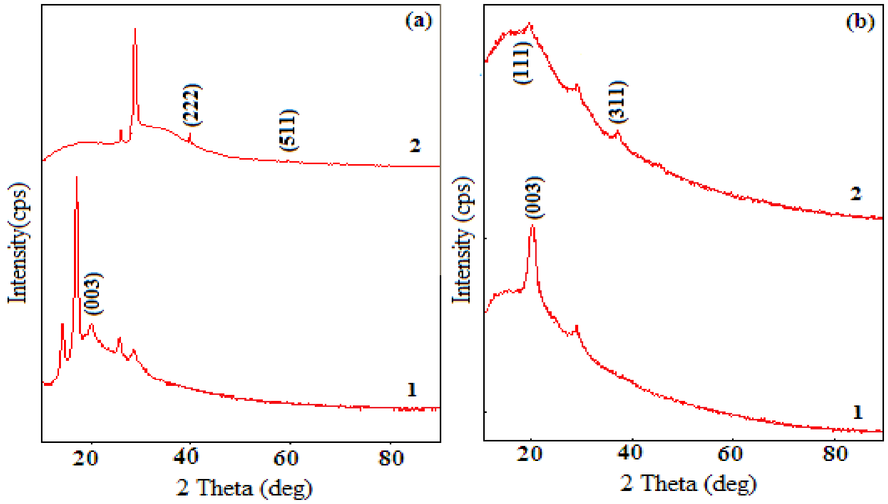

Figure 3. XRD analysis of CoO(OH) (1) and Co_3O_4 (2) films synthesized using (a) 3% and (b) 1% H_2O_2 on a silicon substrate.

Thus, the size of Co_3O_4 NPs synthesized using 1% H_2O_2 was calculated based on the peak corresponding to the (311) plane and found to be 3.98 nm. The size of Co_3O_4 NPs synthesized using 3% H_2O_2 was calculated from the peak corresponding to the (222) plane and found to be 51.89 nm.

The direct band gap (E_g) values of Co_3O_4 thin films deposited on a glass substrate for 60 and 120 cycles using 1% H_2O_2 were found to be 2.1 eV and 3.26 eV, 1.94 eV and 2.50 eV, respectively. For films synthesized using 3% H_2O_2 under the same conditions, E_g values were 1.89 eV and 3.24 eV, and 1.90 eV and 2.17 eV, respectively. The presence of two band gaps is attributed to the ligand-metal charge transfer events: $O^{2-} \rightarrow Co^{3+}$ (E_{g1}) and $O^{2-} \rightarrow Co^{2+}$ (E_{g2})[1]. The observed decrease in E_g values with increasing oxidizing agent

---

[1] Makhlouf S. A. Structural, Electrical and Optical Properties of Co_3O_4 Nanoparticles / S. A. Makhlouf, Z. H. Bakr, K. I. Aly [et al.] // Superlattices and Microstructures, – 2013, 64, – p. 107–117.

concentration may be related to the increase in particle size. The E_g values of Co_3O_4 thin films deposited in 60 cycles on a silicon substrate using 1% and 3% H_2O_2 were calculated to be 1.38 eV and 1.63 eV, respectively.

Study of the properties of Co_3O_4 NPs synthesized by the sonochemical method in the presence of various stabilizers. XRD analysis results of cobalt oxide NPs synthesized using polyvinyl alcohol (PVA) and styrene as stabilizers are presented in Figure 4. The absence of peaks in the X-ray diffractogram of the sample synthesized using PVA before thermal treatment indicates that the obtained product consists of particles with an amorphous structure. After thermal annealing of the samples at 500°C for 4 hours, low-intensity peaks observed at $2\theta=36.71^\circ$, 39.71°, and 54.56° corresponding to the (311), (222), and (422) planes indicate the formation of weakly crystalline Co_3O_4 (JCPDS-00-009-0418). Additionally, the peak observed at $2\theta=33.22^\circ$ corresponding to the (111) plane is attributed to CoO (JCPDS-42-1300), suggesting that the resulting particles consist of two phases. In the X-ray diffractogram of the samples synthesized using styrene before thermal treatment, the peaks observed at $2\theta=33.39^\circ$ and 59.41° corresponding to the (012) and (110) planes are attributed to α-$Co(OH)_2$[2]. After thermal annealing, peaks appeared at 2θ values of 31.34, 36.84, 59.75, and 65.23, corresponding to the (220), (311), (511), and (440) planes, indicating the formation of cubic Co_3O_4. The average crystallite size of Co_3O_4 NPs synthesized using styrene as a stabilizer was calculated to be 7.29 nm. In the diffractogram of the samples synthesized using PVA as a capping agent, the intense peak corresponds to CoO. The average crystallite size estimated for the diffraction peak at $2\theta=33.22$ is 36 nm. Therefore, the possible growth

---

[2] Wang M. Preparation of Self-Assembled Cobalt Hydroxide Nanoflowers and the Catalytic Decomposition of Cyclohexyl Hydroperoxide / M. Wang, J. Ma, C. Chen [et al.] // Journal of Materials Chemistry, –2011, 21, – p. 12609–12612.

mechanism of α-$Co(OH)_2$ can be described by the following equations[3]:

$$NaBH_4 + 2H_2O \rightarrow NaBO_2 + 4H_2$$

$$NaBO_2 + 2H_2O \rightarrow NaOH + H_3BO_3$$

$$Co^{2+} + OH^{-} \rightarrow Co(OH)_2$$

The hydrolysis of an aqueous $NaBH_4$ solution results in the formation of sodium metaborate, and the subsequent hydrolysis of the latter leads to the formation of sodium hydroxide[3].

Figure 5 shows the XRD patterns of cobalt oxide NPs synthesized using 3-MPA at different concentrations. No peaks were observed in the X-ray diffractogram of the samples synthesized using 2% 3-MPT before thermal treatment. After thermal treatment, the peaks observed at $2\theta=31.19^o$, 34.34^o, 36.84^o, 44.92^o, 59.30^o and 65.17^o corresponding to the (220), (111), (311), (400), (511) and (440) planes are attributed to the cubic phases of Co_3O_4 and CoO. In the XRD analysis of the samples synthesized using 7% 3-MPT before thermal treatment, the diffraction peaks correspond to a mixture of $Co(OH)_2$ and cobalt oxyhydroxide (CoOOH). The formation mechanism of CoOOH can be explained by the following equations[4]:

$$H_2O))))))\rightarrow H\cdot + OH\cdot$$

$$H\cdot + H\cdot \rightarrow H_2$$

$$OH\bullet + OH\bullet \rightarrow H_2O_2$$

$$2\,Co(OH)_2 + H_2O_2 \rightarrow 2CoOOH + 2H_2O$$

The average crystallite sizes of Co_3O_4 NPs synthesized using 2% and 7% 3-MPA were 16.26 nm and 6.11 nm, respectively. As seen from the XRD pattern, the intensity of the diffraction peaks decreases with increasing concentration of the stabilizer agent. This is due to the

---

[3] Bashir O. Encapsulation of Silver Nanocomposites and Effects of Stabilizers / O. Bashir, S. Hussain, Z. Khan [et al.] // Carbohydrate Polymers, – 2014, 107, – p.167–173.

[4] Al-Qirby L. M. Sonochemical Synthesis and Characterization of Co_3O_4 Nanocrystals in the Presence of the Ionic Liquid [EMIM][BF_4] / L. M. Al-Qirby, S. Radiman, C. W. Siong [et al.] // Ultrasonics Sonochemistry, –2017, 38, – p. 640–651.

reduction of the particle size. When the amount of stabilizer is low, the stabilization effect is insufficient, leading to rapid aggregation.

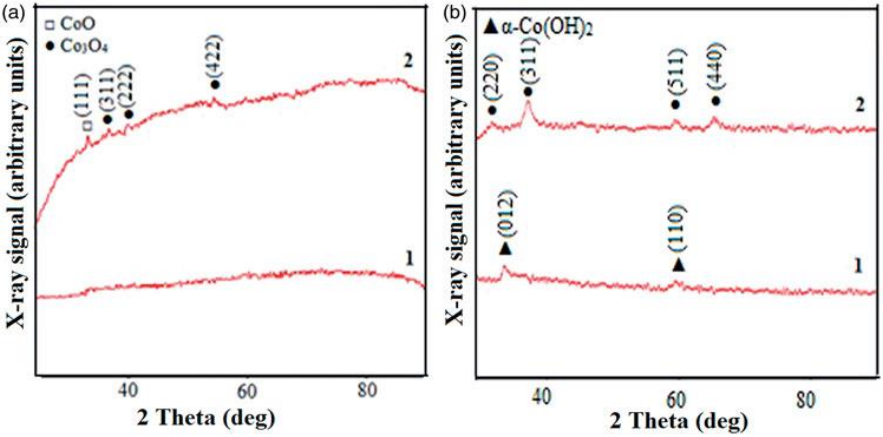

Figure 4. **XRD pattern of NPs synthesized using (a) polyvinyl alcohol and (b) styrene (1) before and (2) after annealing at 500°C in air for 4 h.**

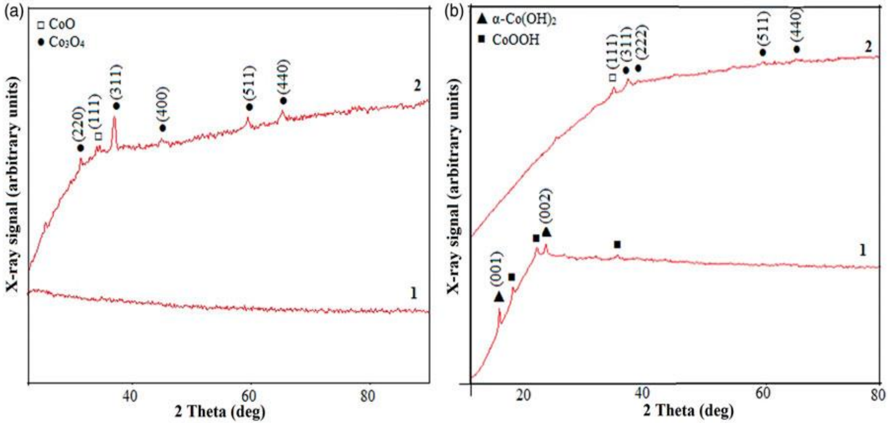

Figure 5. XRD pattern of NPs synthesized using (a) 2% and (b) 7% 3-mercaptopropionic acid before (1) and after annealing at 500°C in air for 4 h (2).

The E_g values were calculated to be 1.75 and 3.10 eV; 2.10 eV and 3.20 eV for oxide NPs synthesized using PVA and styrene, respectively. The different concentrations of 3-MPA influence the

NP size. The E_g values of cobalt oxide NPs synthesized using 2% and 7% 3-MPA were 1.65 eV and 3.55 eV; 1.85 eV and 3.13 eV, respectively. As indicated by the results, the E_g value increases with decreasing nanoparticle size.

Figure 6 shows the IR spectra of the cobalt oxide NPs synthesized using PVA and styrene. In the spectra of samples synthesized using PVA before thermal annealing, a broad band at 3440 cm^{-1} is attributed to the stretching vibration of hydrogen-bonded hydroxyl groups of PVA. The absorption band at 2928 cm^{-1} is assigned to the asymmetric C–H stretching. The bending and wagging vibrations of CH_2 appear at 1443 cm^{-1} and 1340 cm^{-1}, respectively. The band at 1740 cm^{-1} is assigned to the C=O stretching of the acetate group of PVA. The band observed at 1126 cm^{-1} is characteristic of the C–O stretching vibration. Moreover, the peak observed at 676 cm^{-1} is attributed to Co–OH bending. Several of the aforementioned PVA-related peaks either disappeared or decreased in intensity after annealing at 500°C, indicating decomposition of the polymer[5]. After annealing, two sharp peaks appeared at 662 cm^{-1} (υ_1) and 567 cm^{-1} (υ_2), confirming the formation of Co_3O_4. The υ_1 band is attributed to tetrahedrally coordinated Co^{2+} ions, while the υ_2 band is characteristic of octahedrally coordinated Co^{3+} ions[6].

In the spectra of the samples synthesized using styrene before thermal annealing, the band at 2928 cm^{-1} is ascribed to aromatic C–H stretching. The presence of a peak at 1654 $cm^{-1,}$ corresponding to the C=C stretching vibration of the vinyl group, indicates the presence of free styrene in the sample[7]. Peaks observed at 600 cm^{-1} and 519 cm^{-1} are ascribed to Co–OH bending and Co–O stretching

---

[5] Ghafari E. Investigating Process-Structure Relations of ZnO Nanofiber via Electrospinning Method / E. Ghafari, Y. Feng, Y. Liu [et al.] // Composites Part B, –2017, 116, – p. 40–45.

[6] Ozkaya T. Reflux synthesis of Co_3O_4 nanoparticles and its magnetic characterization / T. Ozkaya, T. A.Baykal, M.S.Toprak [et al.] // Journal of Magnetism and Magnetic Materials, – 2009, 321, –p.2145–2149.

[7] Yu Y., Korgel B. A. Controlled Styrene Monolayer Capping of Silicon Nanocrystals by Room Temperature Hydrosilylation // Langmuir, –2015, 31, – p. 6532–6537.

vibrations, respectively. After thermal annealing, two distinct bands appeared at 662 cm^{-1} and 570 cm^{-1}, confirming the formation of Co_3O_4. These findings are in good agreement with the XRD analysis.

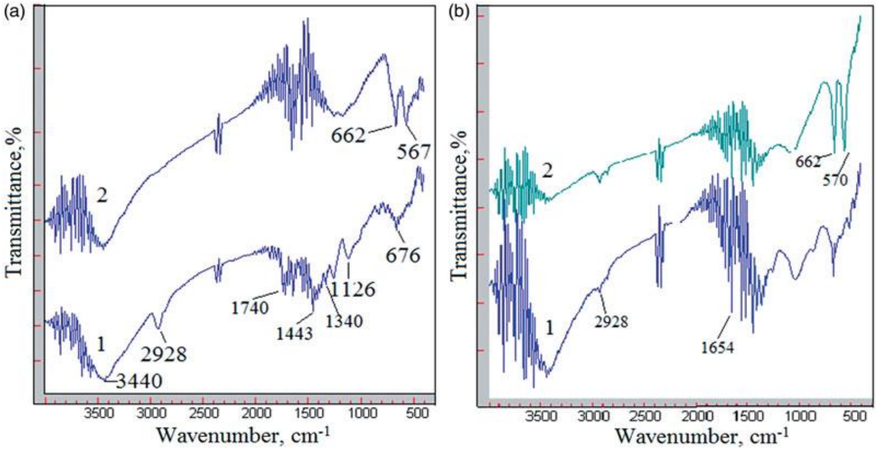

Figure 6. FTIR spectra of samples synthesized using (a) polyvinyl alcohol and (b) styrene before (1) and (2) after thermal annealing at 500°C (2).

Figure 7 presents the FTIR spectra of cobalt oxide NPs synthesized using 3-MPA at different concentrations. In the spectra of samples before thermal annealing, the broad band at 3430 cm^{-1} corresponds to O–H vibrations. In the spectra of the samples synthesized using 7% 3-MPA, peaks at 1707 cm^{-1} and 2928 cm^{-1} are ascribed to the C=O stretching of carboxylic groups and C–H stretching of methylene groups, respectively. The peaks observed at 807 cm^{-1} and 835 cm^{-1} are attributed to C–S bending vibrations in the spectra of the samples synthesized using 7% and 2% 3-MPA, respectively. The bands appearing at 2631 cm^{-1} and 2565 cm^{-1} in the spectrum of the sample synthesized using 7% MPA are due to the free S–H stretching vibration of the thiol group. These characteristic peaks are absent in the spectrum of the sample synthesized with 2% MPA, confirming the covalent bond formation between the thiol group of MPA and the metal atom. In this spectrum, the peak related to C=O stretching disappeared. The new bands at 1560 cm^{-1} and 1420 cm^{-1} correspond to the asymmetric and symmetric stretching vibrations of the carboxylate group (COO$^-$). It indicates that the carboxylate group of MPA also forms a coordination bond with the metal center. Before thermal annealing, the IR spectrum of 7% MPA-capped NP displays stretching COO$^-$ bands at 1527 cm^{-1} and 1406 cm^{-1}. These results suggest that both groups (−SH and −COOH) are partially ligated to the NP surface. In the same sample, the absorption bands at 639 cm^{-1} and 518 cm^{-1} are assigned to the Co–OH bending and Co–O stretching vibrations, respectively. These results coincide with the XRD analysis. These characteristic peaks are observed at 676 cm^{-1} and 519 cm^{-1} for NP capping with 2% MPA. After annealing at 500°C, some of the bands associated with 3-MPA disappeared, which is attributed to its decomposition and evaporation at high temperatures. In the spectrum of the sample capped with 2% 3-MPA, the peaks observed at 661 cm^{-1} and 568 cm^{-1} (in the spectrum of the sample capped with 7% 3-MPA, the peaks observed at 669 cm^{-1} and 568 cm^{-1}) confirm the formation of cobalt oxide[8].

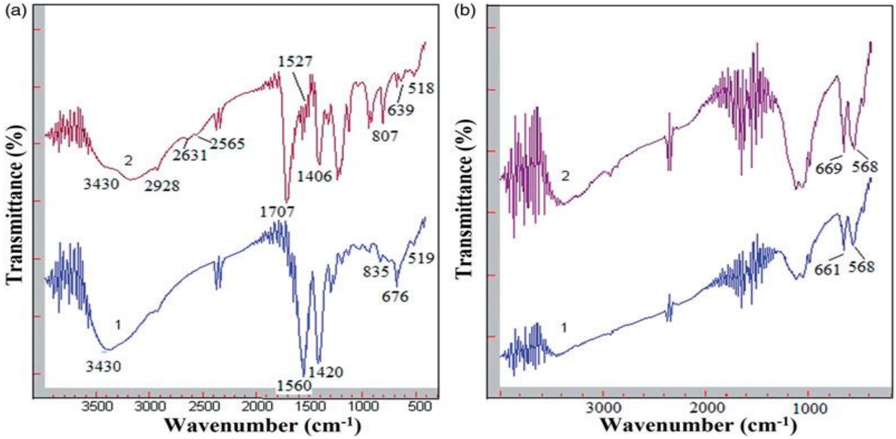

Figure 7. FTIR spectra of samples synthesized using (1) 2%, (2) 7% 3-mercaptopropionic acid before (a) and after thermal annealing at 500°C (b).

---

[8] Mammadyarova S.J. Influence of stabilizing agents on structural and optical properties of cobalt oxide nanoparticles synthesized by an ultrasound-assisted method / S.J.Mammadyarova, M.B.Muradov, A.M.Maharramov [et al.] // Spectroscopy Letters, – 2019, 52(10), – p. 677-686.

Study of the properties of Co_3O_4 NPs synthesized by the sonochemical method and doped with Cu and Ag at various concentrations. Figure 8 shows the XRD patterns of pure and different concentrations of Cu-doped Co_3O_4 NPs after thermal annealing at 500°C for 4h. In the diffractogram of undoped cobalt oxide NPs, low-intensity peaks were observed at $2\theta=18.91^{o}$, 31.25^{o}, 36.84^{o}, 38.56^{o}, 65.19^{o}, corresponding to the (111), (220), (311), (222), and (440) planes. This result is in good accordance with the JCPDS-00-009-0418 standard data and indicates the formation of Co_3O_4 with a cubic crystal structure. The absence of additional diffraction peaks indicates the high purity of the synthesized Co_3O_4 NPs. The average crystallite size of the undoped Co_3O_4 NPs was calculated to be 22.55 nm. For the Cu-doped Co_3O_4 NPs ($Cu_xCo_{3-x}O_4$, x=0.02, 0.04, 0.06, 0.1), the average crystallite sizes were found to be 29.17 nm, 21.87 nm, 34.19 nm, and 31.26 nm, respectively. As evident, the size of the Co_3O_4 NPs varies non-linearly with the increasing concentration of Cu dopant. No peaks related to copper or copper oxides were observed in the diffractograms of the doped samples. This indicates the successful incorporation and dispersion of copper into the Co_3O_4 lattice[9]. Since the ionic radius of Co^{2+} (tetrahedrally coordinated) (0.72 Å) and the ionic radius of Cu^{2+} (tetrahedrally coordinated) (0.71 Å) are close to each other, Cu^{2+} ions can easily enter the lattice sites of Co^{2+} in the Co_3O_4 matrix and replace these ions. In the diffractograms of copper-doped Co_3O_4 NPs, the peaks shifted slightly toward a higher angle and the value of the lattice constant decreased compared to undoped NPs. As the size of the nanoparticles increases, the value of the lattice strain decreases, and conversely, as the size decreases, the value of the lattice strain increases. For more information about the structural characteristics of the nanoparticles, interplanar distance, lattice strain, dislocation density, and unit cell volume were calculated, and the values are listed in Table 1:

---

[9] Mu G. Oxygen Vacancy Defects Engineering on Cu-Doped Co_3O_4 for Promoting Effective COS Hydrolysis / G. Mu, Y. Zeng, Y. Zheng [et al.] // Green Energy & Environment, – 2023, 8, – p. 831-841.

Table 1. The values of crystal structure parameters of undoped and Cu-doped Co_3O_4 NPs ($Cu_xCo_{3-x}O_4$, x=0.02, 0.04, 0.06, 0.1) annealed at 500°C.

Samples	2θ (°)	Crys. size (nm)	Inter-planar distance (Å)	Lattice strain	Dislo-cation density (10^{-3})	Latti-ce cons-tant (Å)	Unit cell volume $(Å)^3$
Co_3O_4	36.84	22.55	2.438	0.0051	1.967	8.085	528.47
$Cu_{0.02}Co_{2.98}O_4$	36.94	29.17	2.431	0.0039	1.175	8.064	524.33
$Cu_{0.04}Co_{2.96}O_4$	36.86	21.87	2.437	0.0052	2.091	8.081	527.71
$Cu_{0.06}Co_{2.94}O_4$	36.94	34.19	2.431	0.0033	0.855	8.064	524.33
$Cu_{0.1}Co_{2.9}O_4$	36.95	31.26	2.431	0.0037	1.023	8.063	524.09

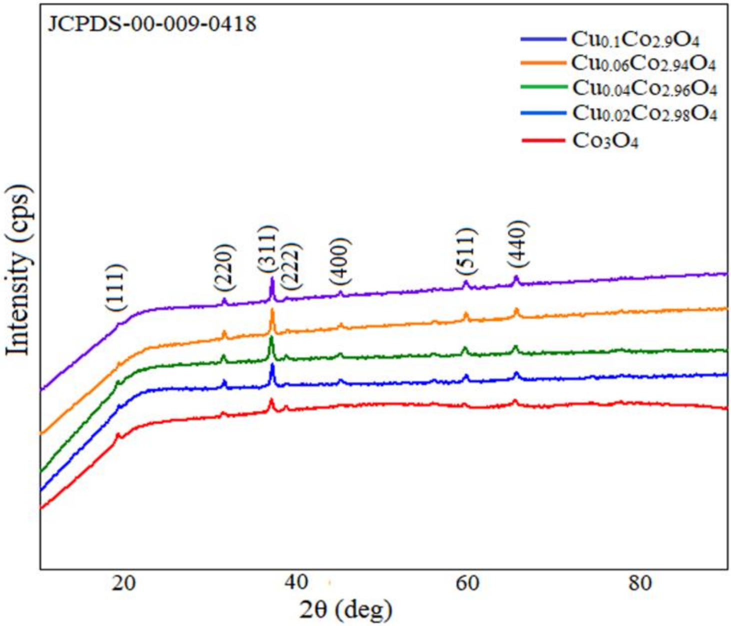

Figure 8. XRD patterns of undoped and Cu-doped Co_3O_4 NPs ($Cu_xCo_{3-x}O_4$, x=0.02, 0.04, 0.06, 0.1) annealed at 500°C.

The XRD patterns of pure and different concentrations of Cu-doped Co_3O_4 NPs after thermal annealing at 600°C for 4h are presented in Figure 9. The peaks observed at 2θ=31.12°, 36.71°, 38.36°, 44.70°, 59.18°, 65.05° values in the diffractogram of undoped NPs correspond to (220), (311), (222), (400), (511), (440) planes, confirming the formation of Co_3O_4. The crystallite size of these NPs calculated by the Debye-Scherrer formula was 22.43 nm. For the Cu doped Co_3O_4 NPs ($Cu_xCo_{3-x}O_4$, x=0.02, 0.04, 0.06, 0.1) thermal annealed at 600°C, the crystallite sizes were determined to be 21.86 nm, 23.7 nm, 21.8 nm, 22.38 nm, respectively. With increasing temperature, the size of Co_3O_4 NPs doped with Cu at x=0.04 increased, while the size of Co_3O_4 NPs doped with Cu at x=0.02, 0.06, and 0.1 decreased.

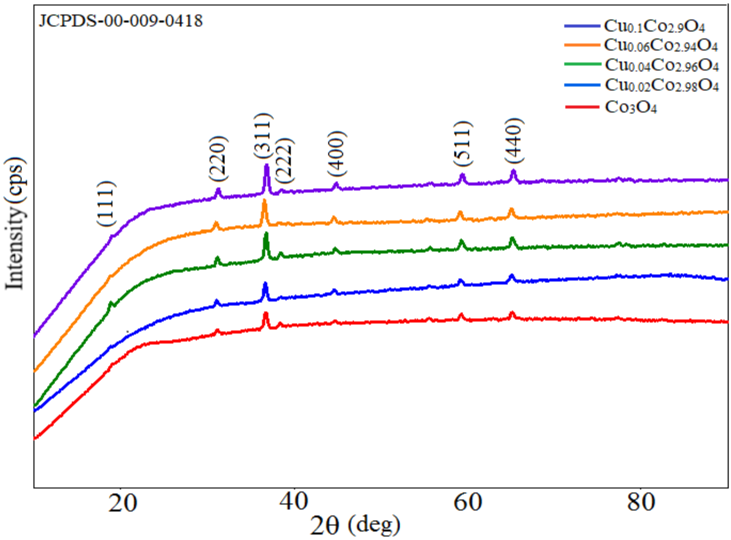

Figure 9. XRD patterns of undoped and Cu-doped Co_3O_4 NPs ($Cu_xCo_{3-x}O_4$, x=0.02, 0.04, 0.06, 0.1) annealed at 600°C.

Figure 10 displays the XRD patterns of pure and different concentrations of Ag-doped Co_3O_4 NPs after thermal annealing at 500°C for 4h. In the diffractogram of the sample doped with Ag at x=0.02, six peaks were observed at 2θ=19.11°, 31.43°, 37.04°, 44.98°, 59.53° and 65.31°, corresponding to (111), (220), (311), (400), (511) and (440) planes belonging to Co_3O_4 with cubic crystal structure. As can be seen from the diffractograms, no peaks of silver or silver (I) oxide (Ag_2O) were detected in the doped samples. In comparison with undoped Co_3O_4, the peak corresponding to the (311) plane shifted to relatively higher angles in Ag-doped NPs. It indicates the presence of local distortions in the Co_3O_4 crystal lattice due to Ag doping. Because the ionic radius of Ag^+ (tetrahedrally coordinated) (1.14 Å) is higher than the ionic radius of Co^{2+} (0.72 Å). The crystallite sizes of Ag-doped Co_3O_4 NPs ($Ag_xCo_{3-x}O_4$, x=0.02, 0.04, 0.06, 0.1) were calculated as 17.17 nm, 19.02 nm, 23.03 nm, and 17.5 nm, respectively. Other crystal structure parameters for these synthesized NPs are listed in Table 2. The size reduction of the Ag-doped NPs at x=0.02 compared to the undoped Co_3O_4 NPs can be attributed to the internal microstructural strain and distortion in the Co_3O_4 lattice by the incorporation of Ag^+ ions. As can be seen from the results, the particle size increased with increasing silver concentration up to x=0.06, while at higher silver concentrations (x=0.1), the size decreased. This can be explained by the fact that as the silver concentration increases, the internal structural weakening increases, which increases the growth rate. However, at higher dopant concentrations, the stability decreases due to increased lattice defects, leading to a reduction in particle size.

Table 2. The values of crystal structure parameters of undoped and Ag-doped Co_3O_4 NPs ($Ag_xCo_{3-x}O_4$, x=0.02, 0.04, 0.06, 0.1) annealed at 500°C.

Samples	**2θ (°)**	**Crys. Size (nm)**	**Inter-planar distance (Å)**	**Lattice strain**	**Dislo-cation density (10^{-3})**	**Latti-ce cons-tant (Å)**	**Unit cell volume (Å)^3**
Co_3O_4	36.84	22.55	2.438	0.0051	1.967	8.085	528.47
$Ag_{0.02}Co_{2.98}O_4$	37.04	17.17	2.425	0.0066	3.392	8.043	520.32
$Ag_{0.04}Co_{2.96}O_4$	36.86	19.02	2.437	0.0060	2.764	8.081	527.73
$Ag_{0.06}Co_{2.94}O_4$	36.89	23.03	2.434	0.0050	1.885	8.073	526.07
$Ag_{0.1}Co_{2.9}O_4$	36.89	17.5	2.434	0.0065	3.265	8.073	526.07

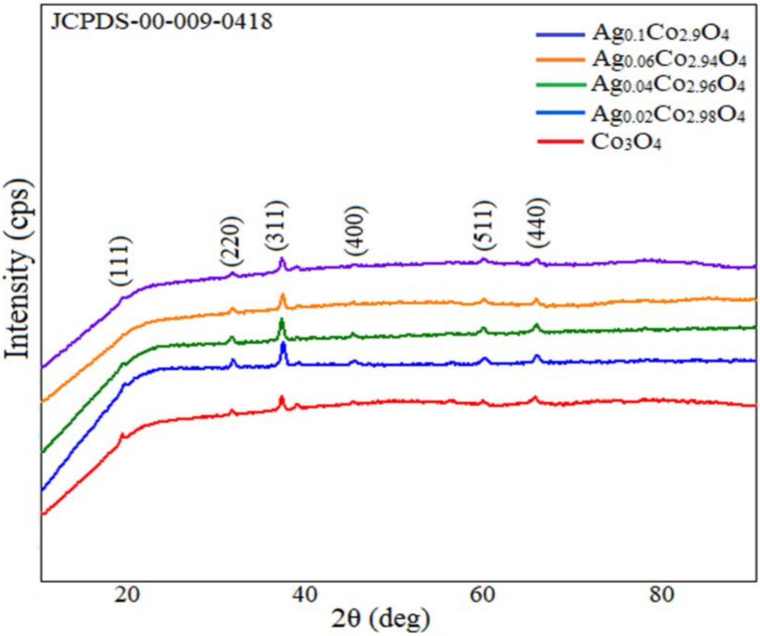

Figure 10. XRD patterns of undoped and Ag-doped Co_3O_4 NPs ($Ag_xCo_{3-x}O_4$, x=0.02, 0.04, 0.06, 0.1) annealed at 500ºC.

The XRD patterns of pure and different concentrations of Ag-doped Co_3O_4 NPs after thermal annealing at 600ºC for 4h are shown in Figure 11. In the diffractogram of sample doped with Ag at x=0.02, the peaks observed at 2θ=18.85º, 30.91º, 36.53º, 44.51º, 59.12º and 64.90º corresponding to (111), (220), (311), (400), (511) and (440) planes belong to Co_3O_4 and the crystallite size of these NPs was calculated to be 24.83 nm. The crystallite sizes of Ag-doped Co_3O_4 NP with doping levels of x=0.04, 0.06, and 0.1 were 21.87 nm, 20.82 nm, and 23.84 nm, respectively, after annealing at the same temperature. Thus, the crystallite size decreased at x=0.06, while it increased at x=0.04 and 0.1 with increasing annealing temperature.

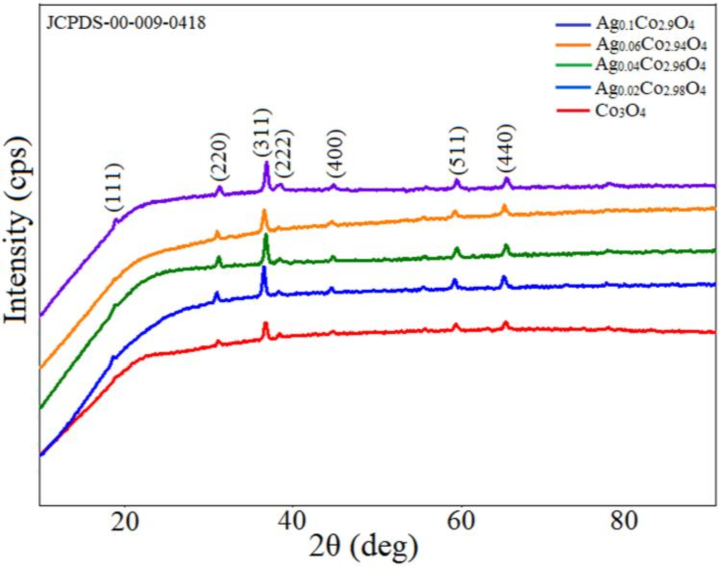

Figure 11. XRD patterns of undoped and Ag-doped Co_3O_4 NPs ($Ag_xCo_{3-x}O_4$, x=0.02, 0.04, 0.06, 0.1) annealed at 600ºC.

The direct E_g values for the samples were determined by extrapolation the linear portion of the $(\alpha h\nu)^2$ versus hν plot to the x-axis, and the results are presented in Table 3. As observed, Cu doping at x=0.02 caused the E_g value of Co_3O_4 NPs annealed at 500ºC to increase from 1.58 eV and 3.33 eV to 1.70 eV and 3.43 eV. The reason for this increase can be explained by the Moss-Burstein effect. The decrease in the E_g value at high copper concentrations is associated with crystal defects.

For Cu doped samples annealed at 600ºC, the E_g value increases with decreasing NP size, which is consistent with the quantum size effect. The increase in E_g values for Ag-doped samples annealed at 500ºC and 600ºC, compared to undoped Co_3O_4 NPs, is explained by the Moss-Burstein effect.

Table 3. The E_g values for undoped and doped Co_3O_4 NPs with different concentrations of Cu and Ag annealed at 500°C and 600°C.

Samples	**E_g (eV)** (500°C)	**E_g (eV)** (600°C)
Co_3O_4	1.58 və 3.33	1.20 və 3.25
$Cu_{0.02}Co_{2.98}O_4$	1.70 and 3.43	1.66 and 3.30
$Cu_{0.04}Co_{2.96}O_4$	1.45 and 3.26	1.14 and 3.20
$Cu_{0.06}Co_{2.94}O_4$	1.44 and3.21	1.70 and 3.30
$Cu_{0.1}Co_{2.9}O_4$	1.26 and 3.08	1.56 and 3.27
$Ag_{0.02}Co_{2.98}O_4$	1.69 and 3.35	1.50 and 3.27
$Ag_{0.04}Co_{2.96}O_4$	1.60 and 3.26	1.52 and 3.30
$Ag_{0.06}Co_{2.94}O_4$	1.72 and3.47	1.72 and 3.26
$Ag_{0.1}Co_{2.9}O_4$	1.74 and 3.44	1.70 and 3.26

According to TEM images of undoped Co_3O_4 NPs annealed at 500°C, these NPs have spherical-like, hexagonal-like and irregular morphology, and their sizes range from 5.57 nm to 79.15 nm. Co_3O_4 NPs doped with Cu at x=0.1 have spherical-like, hexagonal, rhombohedral-like, and irregular morphology, and their sizes range from 15.78 nm to 78.31 nm. Co_3O_4 NPs doped with Ag at x=0.1 have rhombohedral-like, hexagonal, and spherical morphology, and their sizes range from 8.30 nm to 73.75 nm.

The photocatalytic activity of pure Co_3O_4 and different concentrations of Cu and Ag-doped Co_3O_4 nanoparticles was investigated on methylene blue (MB) dye under visible light irradiation. According to the Beer-Lambert law, the concentration of a dye solution is proportional to its absorbance. Therefore, the degradation efficiency was calculated from the following equation[10]:

$$R\ (\%) = \frac{C_0 - C}{C_0} \cdot 100\% = \frac{A_0 - A}{A_0} \cdot 100\%$$

---

[10] Singh R., Barman P.B., Sharma D. Synthesis, structural and optical properties of Ag doped ZnO nanoparticles with enhanced photocatalytic properties by photodegradation of organic dyes // J. Mater. Sci. Mater. Electron, – 2017, 28, – p. 5705–5717.

Here, C_0 and A_0 represent the initial concentration and absorbance of the dye solution, while C and A denote the concentration and absorbance after a specific time interval, respectively.

According to the experimental results, the degradation efficiency for MB dye was 79.20% after 330 minutes in the presence of pure Co_3O_4 nanoparticles and an oxidizing agent (H_2O_2). Only minimal degradation (2.72%) was observed in the absence of a catalyst under the same conditions. The degradation efficiency in the presence of $Cu_{0.02}Co_{2.98}O_4$ NPs increased to 87.51% after that time. The degradation efficiency after 330 minutes in the presence of $Cu_{0.04}Co_{2.96}O_4$, $Cu_{0.06}Co_{2.94}O_4$, and $Cu_{0.1}Co_{2.9}O_4$ NPs was 74.66%, 85%, and 65.60%, respectively. The decrease of photocatalytic activity at high concentrations of copper can be attributed to the excessive oxygen vacancies and the high amount of the dopant acting as recombination centers of photoinduced electrons and holes[11].

Study of the properties of NiO NPs synthesized by the sonochemical method and doped with Cu and Ag at various concentrations. Figure 12 shows the XRD patterns of pure and different concentrations (2%, 4%, 6%, and 10%) of Cu-doped NiO NPs after thermal annealing at 400°C for 2h. Five broad diffraction peaks were observed at $2\theta=37.40^o$, 43.36^o, 62.98^o, 75.42^o, and 79.58^o in the diffractogram of the undoped sample. The (111), (200), (220), (311), and (222) planes corresponding to these diffraction angles indicate the formation of face-centered cubic NiO. These results are consistent with JCPDS #47-1049. The size, interplanar distance, and lattice constant of NiO NPs were calculated from the peaks corresponding to the (111) and (200) planes and are summarized in Table 4, along with other structural parameters.

---

[11] Hameeda B. Development of Cu-doped NiO nanoscale material as efficient photocatalyst for visible light dye degradation / B. Hameeda, A. Mushtaq, M. Saeed [et al.] // Toxin Rev., – 2021, 40, – p. 1396–1406.

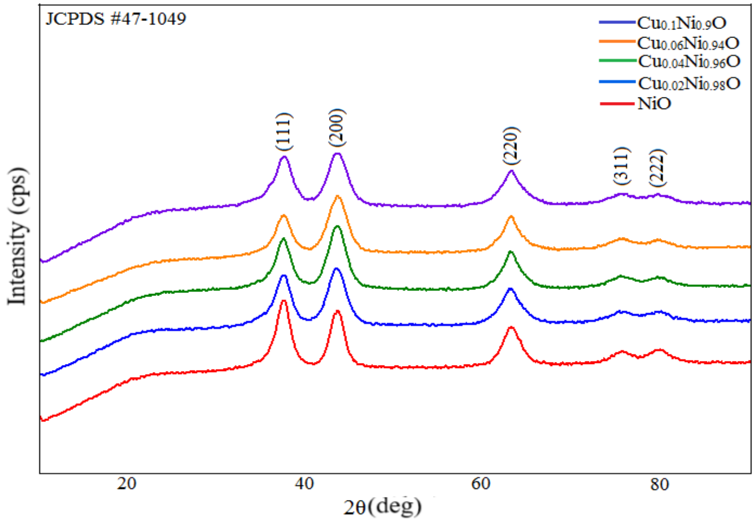

Figure 12. XRD patterns of undoped and 2%, 4%, 6%, 10% Cu-doped NiO NPs annealed at 400°C.

Table 4. The values of crystal structure parameters of undoped and 2%, 4%, 6%, 10% Cu-doped NiO NPs annealed at 400°C.

Samples	**2θ (°)**	**Crys. size (nm)**	**Inter-planar distance (Å)**	**Lattice strain**	**Dislo-cation density (10^{-2})**	**Lat-tice cons-tant (Å)**	**Unit cell volume (Å)^3**
NiO	37.40	4.59	2.403	0.0246	4.747	4.161	72.06
	43.36	4.91	2.085	0.0200	4.148	4.170	72.53
$Cu_{0.02}Ni_{0.98}O$	37.35	3.78	2.406	0.0300	6.999	4.167	72.34
	43.17	3.64	2.094	0.0270	7.547	4.188	73.44
$Cu_{0.04}Ni_{0.96}O$	37.35	4.21	2.406	0.0269	5.642	4.167	72.34
	43.33	3.92	2.087	0.0250	6.508	4.173	72.67
$Cu_{0.06}Ni_{0.94}O$	37.32	4.15	2.408	0.0273	5.806	4.170	72.51
	43.41	3.55	2.083	0.0276	7.935	4.166	72.29
$Cu_{0.1}Ni_{0.9}O$	37.37	3.46	2.404	0.0326	8.353	4.165	72.23
	43.21	3.42	2.092	0.0288	8.550	4.184	73.25

Figure 13 displays the XRD patterns of pure and different concentrations (2%, 4%, 6%, and 10%) of Ag-doped NiO NPs after thermal annealing at 400°C for 2h. As can be seen from the diffractograms, no peaks related to silver or silver (I) oxide (Ag_2O) were observed in these samples. NiO NPs doped with 2%, 4%, and 10% Ag crystallized with the preferred (200) orientation, while NiO NPs doped with 6% Ag crystallized with the preferred (111) orientation. The size, interplanar spacing, and lattice constant of these NPs were determined based on the peaks corresponding to the (111) and (200) planes and are given in Table 5, along with other crystal structure parameters.

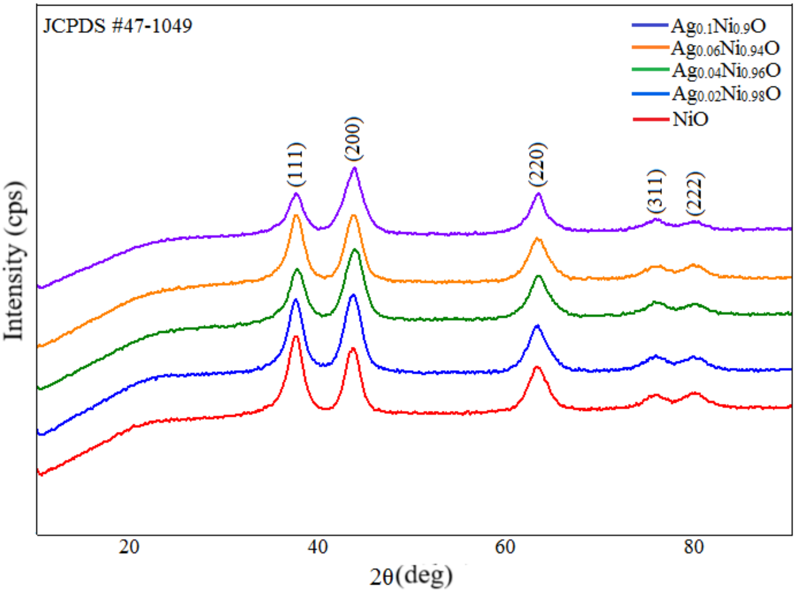

Figure 13. XRD patterns of undoped and 2%, 4%, 6%, 10% Ag-doped NiO NPs annealed at 400°C.

Table 5. The values of crystal structure parameters of undoped and 2%, 4%, 6%, 10% Cu-doped NiO NPs annealed at 400°C.

Samples	**2θ (°)**	**Crys. size (nm)**	**Inter-planar distance (Å)**	**Lattice strain**	**Dislo-cation density (10^{-2})**	**Lattice constant (Å)**	**Unit cell volu-me (Å)^3**
NiO	37.40	4.59	2.403	0.0246	4.747	4.161	72.06
	43.36	4.91	2.085	0.0200	4.148	4.170	72.53
$Ag_{0.02}Ni_{0.98}O$	37.44	4.69	2.400	0.0241	4.546	4.157	71.84
	43.41	4.32	2.083	0.0227	5.358	4.166	72.29
$Ag_{0.04}Ni_{0.96}O$	37.55	4.30	2.393	0.0262	5.408	4.145	71.24
	43.60	3.97	2.074	0.0245	6.345	4.148	71.39
$Ag_{0.06}Ni_{0.94}O$	37.46	4.60	2.399	0.0245	4.726	4.155	71.73
	43.50	4.36	2.079	0.0224	5.260	4.158	71.86
$Ag_{0.1}Ni_{0.9}O$	37.50	4.41	2.396	0.0256	5.142	4.151	71.51
	43.58	3.72	2.075	0.0262	7.226	4.150	71.49

The E_g values for undoped and 2%, 4%, 6%, and 10% Cu-doped NiO NPs were calculated to be 3 eV, 3.11 eV, 3.08 eV, 3.09 eV, and 3.11 eV, respectively. For Ag-doped NiO NPs ($Ag_xNi_{1-x}O$, x=0.02, 0.04, 0.06, 0.1), the E_g values were calculated to be 2.95 eV, 3.10 eV, 3.05 eV, and 3.15 eV, respectively. The slight difference in the E_g values is attributed to the similar sizes of the NPs.

Figure 14 reveals TEM and selected area electron diffraction (SAED) images of undoped NiO NPs annealed at 400°C. As can be seen, the particles have a spherical morphology and tend to agglomerate. The size of the nanoparticles is in the range of 3.24 nm - 12.09 nm. The SAED analysis image consists of several diffraction rings, which indicates that the synthesized NPs have a polycrystalline structure. According to TEM images of 10% Cu and Ag-doped NiO NPs annealed at 400ºC (Figure 15), the particle sizes range from 7.59 nm to 47.87 nm and from 3.04 nm to 16.34 nm, respectively.

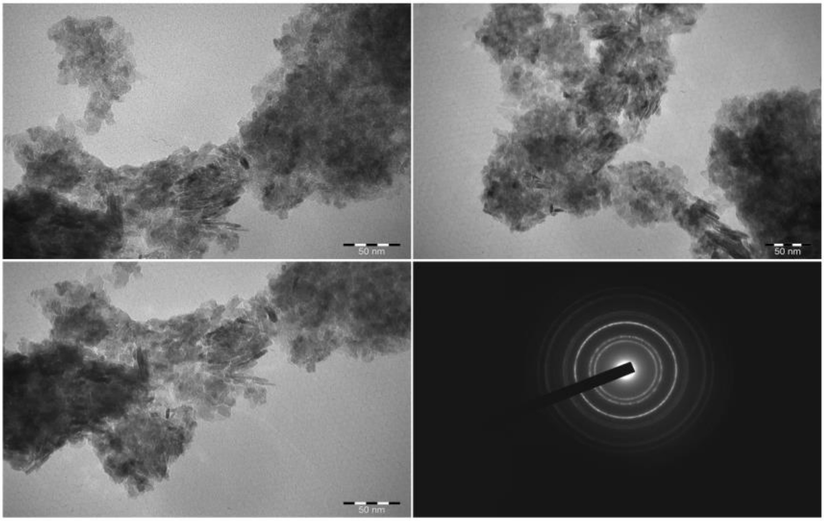

Figure 14. TEM and SAED analysis of undoped NiO NPs thermal annealed at 400ºC.

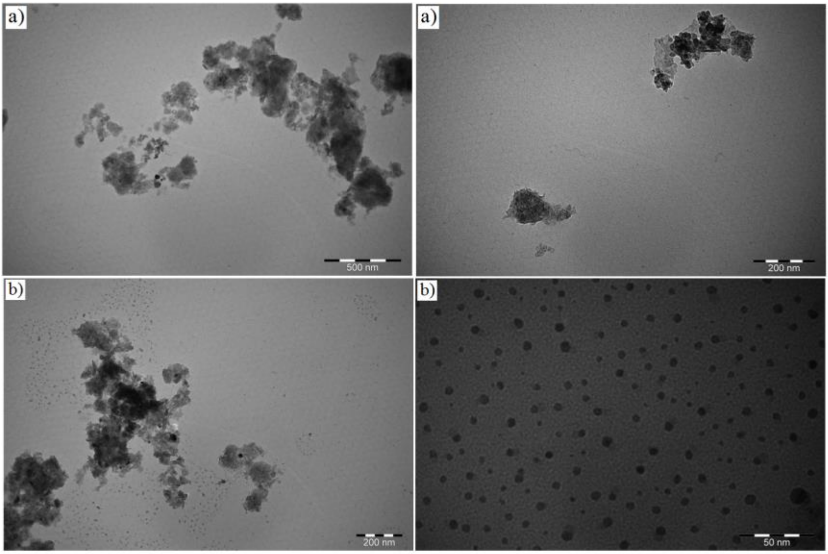

Figure 15. TEM images of NiO NPs doped with 10% a) Cu and b) Ag annealed at 400ºC.

The degradation efficiency for MB dye in the presence of undoped NiO nanoparticles under light exposure was 34.01% after 5 hours. In the presence of NiO NPs doped with high concentrations of copper (6% and 10%), no degradation of the dye was observed over time. In the presence of $Cu_{0.02}Ni_{0.98}O$ NPs, the degradation efficiency was 25.40% after 5 hours. For $Cu_{0.04}Ni_{0.96}O$ NPs, the degradation efficiency was 13.91% after 3 hours, with no further degradation observed beyond this period. In the presence of $Ag_{0.1}Ni_{0.9}O$ NPs, no degradation occurred, while in the presence of $Ag_{0.02}Ni_{0.98}O$, $Ag_{0.04}Ni_{0.96}O$, and $Ag_{0.06}Ni_{0.94}O$ NPs, the efficiency was 43.91%, 30.59%, and 43.83%, respectively, after 5 hours.

Nanocomposites of undoped Co_3O_4 and NiO NPs, as well as those doped with low ($x = 0.02$) and high ($x = 0.1$) concentrations of Cu and Ag, were prepared with PVA and the dependence of the dielectric constant (ε') on frequency at different temperatures (25°C, 40°C, 60°C, 80°C, 100°C) was studied. For all samples, an increase in the value of the dielectric constant was observed with an increase in temperature from 25°C to 100°C. For all samples, a decrease in the dielectric constant was observed with an increase in frequency and then reached an almost constant value in the high-frequency range. This change was explained by the Maxwell-Wagner model.

Study of nickel/nickel oxide nanochains synthesized by oxidation-reduction method. According to the XRD results of Ni nanochains synthesized under the influence of a 25 mT magnetic field for a reaction time of 30 min., three peaks were observed at 2θ values of 44.33º, 52.07º, and 76.57º (Figure 16). The diffraction peaks with (111), (200), and (220) Miller indices corresponding to these degrees belong to Ni nanocrystals with a face-centered cubic structure (JCPDS- 04-0850). After thermal annealing of these samples at 400ºC, three additional peaks with low intensity were observed at 2θ values of 37.10º, 43.14º, and 62.71º. The diffraction peaks with (111), (200), and (220) Miller indices corresponding to these degrees belong to NiO with a face-centered cubic structure (JCPDS #47-1049). This indicates that the surface of Ni nanochains is covered with small-sized NiO. In this diffractogram, the intensity of the peaks belonging to nickel increased and the width of the peak decreased. This is due to the increase in particle size at high temperatures. When the temperature was increased to 600ºC, the intensity of the peaks related to nickel decreased, while the intensity of the peaks related to nickel oxide increased, and the particle size was estimated to be 15.33 nm based on the peak observed at 43º for NiO. Similar properties were also observed for the samples synthesized at 42 mT and 81 mT magnetic fields (Figure 17). The calculated average crystallite sizes and E_g values for the samples synthesized under the influence of different external magnetic fields are summarized in Table 6. The crystallite size was calculated for Ni and NiO separately based on the most intense peak in the diffractogram. As can be seen from the results, the average size of Ni NPs in the nanochain decreased with increasing magnetic force. After oxidation of the samples at 600ºC, the size of NiO formed on the surface of Ni nanochains increased with increasing magnetic force. This is due to the faster oxidation of small-sized particles due to high surface energy. The second reason for such an increase may be the aggregation of particles among themselves.

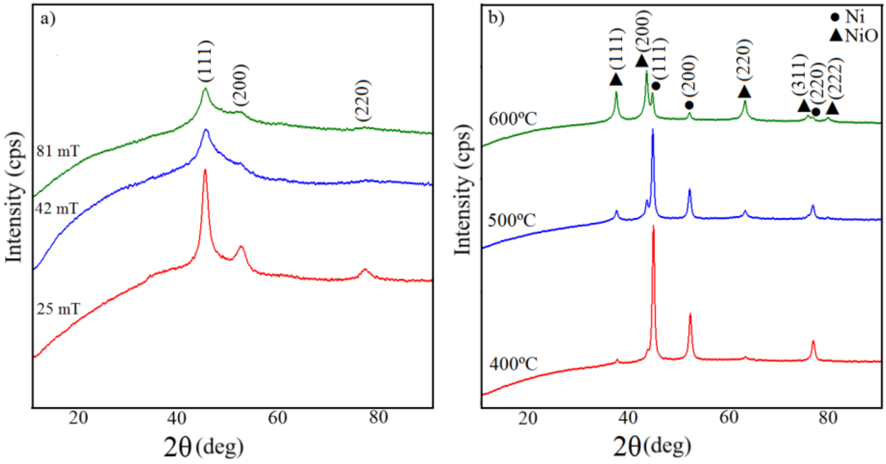

Figure 16. XRD patterns of a) Ni nanochains synthesized under different magnetic fields and b) Ni/NiO nanochains synthesized at 25 mT magnetic field.

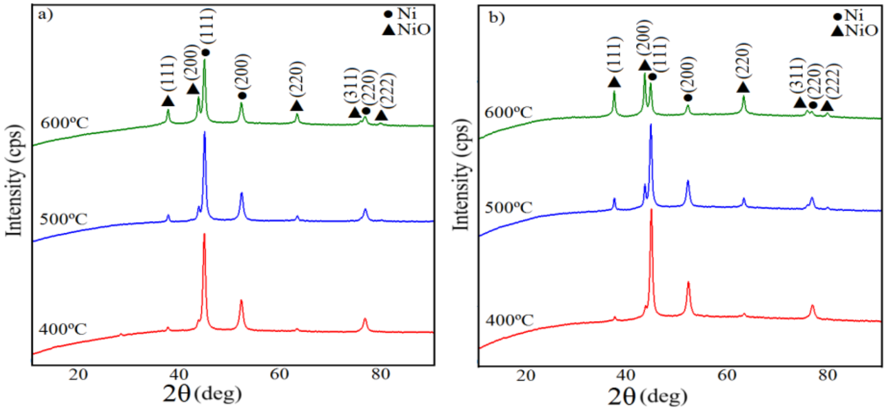

Figure 17. XRD patterns of Ni/NiO nanochains synthesized at a) 42 mT and b)81 mT magnetic field.

Table 6. Crystallite size and band gap value of samples synthesized under external magnetic fields.

Magnetic field intensity	Sample name	Phase	2θ (°)	Crystallite size from XRD (nm)	E_g (eV)
25 mT	As-prepared Ni	Ni	44.33	5.82	-
	Ni/NiO 400°C	Ni	44.30	18.37	3.81
		NiO	43.14	16.84	
	Ni/NiO 500°C	Ni	44.17	19.31	3.99
		NiO	43.05	15.38	
	Ni/NiO 600°C	Ni	44.13	20.36	3.67
		NiO	42.9	15.33	
42 mT	As-prepared Ni	Ni	44.49	1.98	-
	Ni/NiO 400°C	Ni	44.22	16.41	3.97
		NiO	37.07	11.67	
	Ni/NiO 500°C	Ni	44.28	17.4	3.93
		NiO	43.11	23	
	Ni/NiO 600°C	Ni	44.22	18.44	3.95
		NiO	43.12	20.76	
81 mT	As-prepared Ni	Ni	44.05	2.19	-
	Ni/NiO 400°C	Ni	44.22	17.74	3.86
		NiO	43.07	25.5	
	Ni/NiO 500°C	Ni	44.14	19.06	4.0
		NiO	42.97	25.71	
	Ni/NiO 600°C	Ni	44.08	20.35	3.87
		NiO	42.90	24.77	

According to the SEM analysis results (Figure 18), well-dispersed spherical NPs with an average size ranging from 38.3 nm to 64.9 nm were observed after a reaction time of 10 minutes, even under the influence of a magnetic field. However, when the reaction continued for 30 min, Ni particles with an average diameter of 56.1 nm - 88.6 nm coalesced to form linear nanochains, and the chain length was approximately 6.92 µm. After the oxidation of Ni nanochains at 400ºC, the diameter of the nanochains increased to about 68.8-103 nm due to the formation of nickel oxide on the surface of nickel. According to the TEM analysis results, the diameter of Ni/NiO nanochains after oxidation at 600ºC is in the range of 97 nm -133 nm.

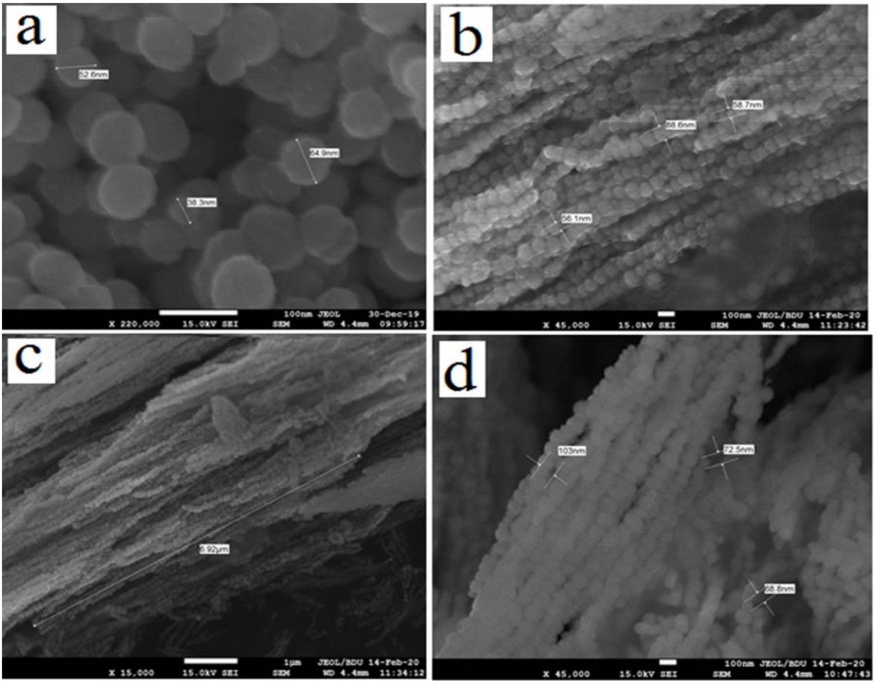

Figure 18. SEM images of products synthesized at 25 mT external magnetic field (a) at 10 min reaction time; (b) and (c) at 30 min reaction time; (d) after oxidation at 400 ◦C.

RESULTS

1. Co_3O_4 thin films were synthesized on two different substrates (glass and silicon) by the SILAR method. It was found that the substrates used affected the structure of the NPs formed. When glass was used as the substrate, NPs formed on its surface had an amorphous structure. When using silicon that had been cleaned of its surface oxide layer as a substrate, poorly crystalline Co_3O_4 NPs were formed on its surface [4-5].
2. Co_3O_4 NPs were synthesized by the sonochemical method in the presence of various stabilizers and it was found that these stabilizers affected the size and optical properties of the NPs. The direct band gap values of the oxide nanoparticles synthesized using PVS, 3-MPT, and styrene as stabilizers was found to be 1.75 eV and 3.10 eV; 1.65 eV and 3.55 eV; 2.10 eV and 3.20 eV, respectively. The differences in the size of the NPs can be attributed to the polar or non-polar nature of the stabilizers used, as well as their various molecular weights and spatial structures [6-7].
3. The synthesis of Co_3O_4 NPs doped with Cu and Ag of different concentrations by the sonochemical method was carried out for the first time. Although there were differences in the NP size and band gap values, no new diffraction peaks were formed. This is explained by the incorporation of dopants into the crystal lattice [17-21].
4. Cu and Ag-doped Co_3O_4 NPs were used as catalysts for the degradation of methylene blue dye under visible light irradiation. The highest degradation efficiency (87.51%) was observed in the presence of $Cu_{0.02}Co_{2.98}O_4$ NPs. When using these NPs as catalysts, the reduction of electron-hole pair recombination and the formation of free electrons and holes for the formation of radicals lead to an increase in the degradation efficiency [17].
5. The synthesis of NiO NPs doped with Cu and Ag of different concentrations by the sonochemical method was carried out for the first time. In this case, the slight difference in the band gap values of the NPs is attributed to their similar particle sizes. When

these NPs were used as catalysts for the photodegradation of methylene blue dye under visible light irradiation, an increase in degradation efficiency was observed in the presence of $Ag_{0.02}Ni_{0.98}O$ compared to undoped NiO NPs [9].

6. Ni nanochains were synthesized under the influence of a magnetic field and then Ni/NiO nanochains were obtained by oxidizing the surface at various temperatures. The diameter of the Ni/NiO nanochain increased with increasing temperature, which was associated with the oxidation process. According to the SEM and TEM results, the diameter of the Ni/NiO nanochains thermally treated at 400°C ranged from 68.8 nm to 103 nm, while those treated at 600°C ranged from 97 nm to 133 nm [8].

Published scientific works on the topic of the dissertation:

1. Mammadyarova S.J., Muradov M.B., Maharramov A.M., Eyvazova G.M. Synthesis and optical characterization of Co_3O_4 thin films // II International scientific conference of young researchers, – Baku: – 27-28 April, – 2018, – p.184-186.
2. Mammadyarova S.J., Muradov M.B., Maharramov A.M., Eyvazova G.M., Balayeva O.O., Aghamaliyev Z.A., Gahramanli L.R. Synthesis of Co_3O_4 thin films by SILAR method at different substrates // 5th International Conference "Nanotechnologies", – Tbilisi: 19-22 November, –2018, –p.121.
3. Mammadyarova S.J., Muradov M.B., Maharramov A.M., Aliyeva A.A. Synthesis of CoO and Co_3O_4 nanoparticles by sonochemical method // 1st International science and engineering conference, – Baku: – 29-30 November, –2018, – p.62-63.
4. Məmmədyarova S.C. Oksidləşdiricinin qatılığının Co_3O_4 nazik təbəqələrinin formalaşmasına təsiri / S.C.Məmmədyarova, M.B.Muradov, A.M.Maharramov [və b.] // Bakı Universitetinin xəbərləri. Təbiət elmləri seriyası, –2018. №2, –s.11-19.
5. Mammadyarova S.J. Characterization of Co_3O_4 thin films synthesized by SİLAR method / S.J.Mammadyarova, M.B.Muradov, A.M.Maharramov [et al.] // Journal of Baku Engineering University. Physics, –2018. 2 (2), – p.87-94.
6. Mammadyarova S.J. Structural and optical characterization of cobalt oxide synthesized by sonochemical method / S.J.Mammadyarova, M.B.Muradov, A.M.Maharramov [et al.] // Journal of Low Dimensional Systems, –2019. 3 (1), – p.4-8.
7. Mammadyarova S.J. Influence of stabilizing agents on structural and optical properties of cobalt oxide nanoparticles synthesized by an ultrasound-assisted method / S.J.Mammadyarova, M.B.Muradov, A.M.Maharramov [et al.] // Spectroscopy Letters, – 2019. 52(10), – p.677-686.

8. Mammadyarova S.J. Synthesis and Characterization of Ni/NiO nanochains / S.J.Mammadyarova, M.B.Muradov, A.M.Maharramov [et al.] // Materials Chemistry and Physics, – 2021. 259, – p.1-7.
9. Mammadyarova S.J. The synthesis methods of nickel oxide nanostructures–a brief review // Вестник НЯЦ РК, – 2021. 1 (85), – p.73-82.
10. Mammadyarova S.J. Synthesis and characterization of cobalt oxide nanostructures- a brief review // Azerbaijan Chemical Journal, – 2021. № 2, – p.80-93.
11. Mammadyarova S.J. The properties of nickel oxide nanostructures-a brief review // Bakı Universitetinin xəbərləri. Fizika-riyaziyyat elmləri seriyası, – 2021. №4, – s.78-85.
12. Mammadyarova S.J., Muradov M.B., Eyvazova G.M., Aghamaliyev Z.A., Balayeva O.O. The effect of magnetic field on structural and optical properties of Ni/NiO nanochains // 2nd International Conference on Light and Light-Based Technologies: ICLLT-2021, – Ankara: –26-28 May, – 2021, – p.107.
13. Mammadyarova S.J., Muradov M.B., Eyvazova G.M., Balayeva O.O. Structural and optical properties of cobalt oxide nanoparticles stabilized with 3-mercaptopropionic acid // 1st International Symposium on Recent Advances in Fundamental and Applied Sciences (ISFAS-2021), – Erzurum: –10-12 September, –2021, – p.180.
14. Mammadyarova S.J., Muradov M.B., Maharramov A.M., Eyvazova G.M., Aghamaliyev Z.A., Balayeva O.O. Structural and optical characterization of Ni/NiO nanochains // 6th International Conference "Nanotechnology" (GTUnano20), –Tbilisi: – 4-7 October, –2021, – p.82.
15. Muradov M.B., Mammadyarova S.J., Eyvazova G.M., Balayeva O.O. Synthesis of Ag-doped Co_3O_4 nanoparticles by sonochemical method // 7th International Conference MTP-2021: Modern Trends in Physics, –Baku: –15-17 December, –2021, – p.76-77.

16. Muradov M.B., Mammadyarova S.J., Eyvazova G.M., Balayeva O.O. Synthesis of copper doped cobalt oxide nanoparticles by sonochemical method // Cukurova 8th International Scientific Researches Conference, – Adana: –15-17 April, –2022, – p.720.
17. Muradov M.B. The effect of Cu doping on structural, optical properties and photocatalytic activity of Co_3O_4 nanoparticles synthesized by sonochemical method / M.B. Muradov, S.J. Mammadyarova, G.M. Eyvazova [et al.] // Optical Materials, – 2023. 142, – p.1-15.
18. Muradov M.B. Sonochemical synthesis and characterization of structural, optical and dielectric properties of Ag-doped Co_3O_4 nanoparticles / M.B. Muradov, S.J. Mammadyarova, G.M. Eyvazova [et al.] // Journal of Cluster Science, –2023. – p.1-17.
19. Mammadyarova S.J., Muradov M.B., Eyvazova G.M., Balayeva O. O. Sonochemical synthesis of Cu-doped Co_3O_4 nanoparticles for photocatalytic degradation of methylene blue // Nanoscience & Nanotechnology Conference, –Rome: –29 May-1 June, –2023, – p.99-101.
20. Mammadyarova S.J., Muradov M. B., Eyvazova G.M., Balayeva O. O. Synthesis of Ag-doped Co_3O_4 nanoparticles by sonochemical method // 8th International Conference: "MTP-2023" Modern Trends in Physics, –Baku: –30 November - 1 December, –2023, – p.35-36.
21. Muradov M.B. Synthesis of $Cu_xCo_{3-x}O_4$ nanoparticles by sonochemical method and characterization of structural, optical properties and photocatalytic activity for the degradation of methylene blue / M.B.Muradov, S.J.Mammadyarova, G.M. Eyvazova [et al.] // RSC Advances, –2024. 14, – p.1082-1093.

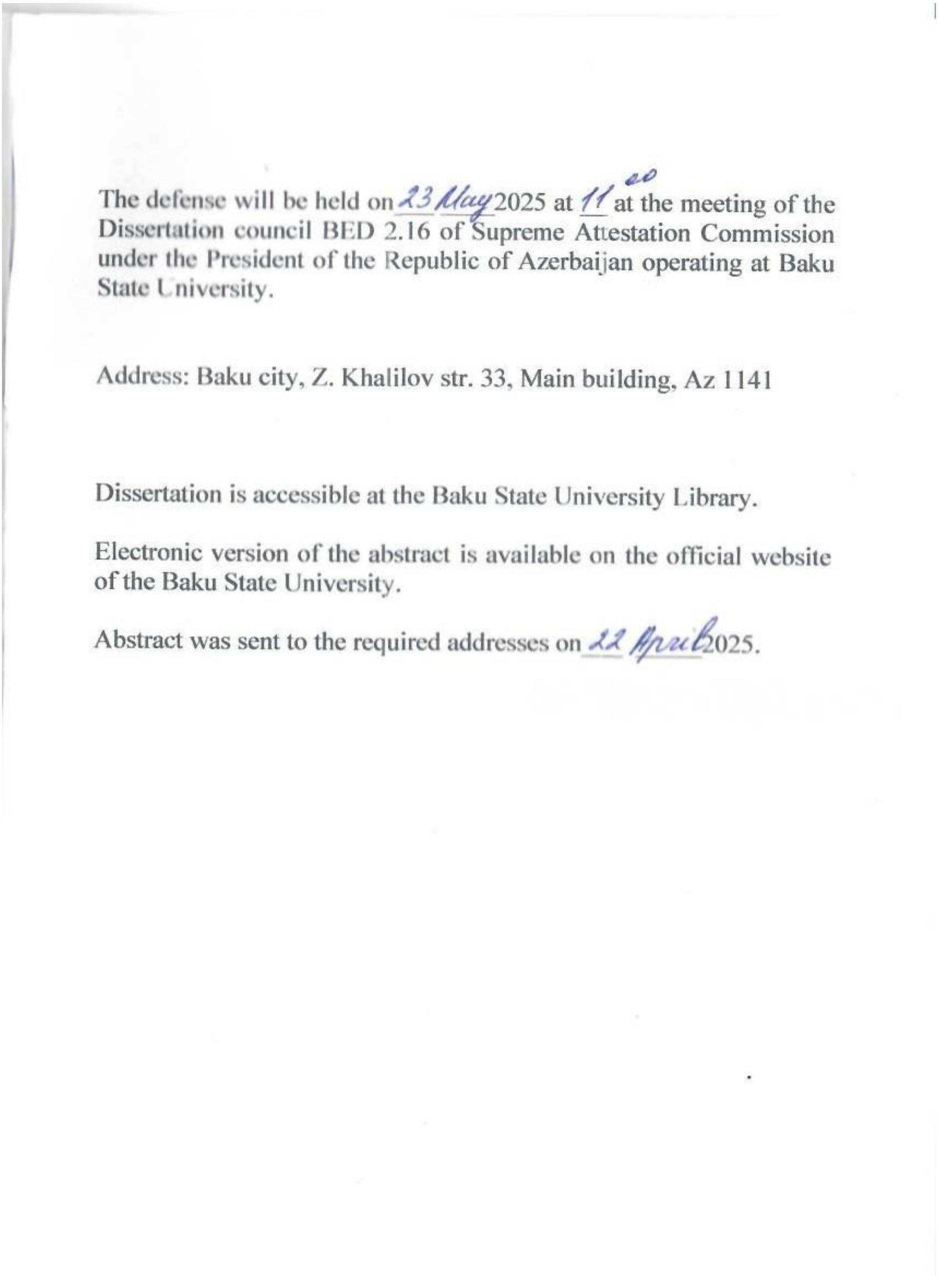

The defense will be held on 23 May 2025 at 11^{00} at the meeting of the Dissertation council BED 2.16 of Supreme Attestation Commission under the President of the Republic of Azerbaijan operating at Baku State University.

Address: Baku city, Z. Khalilov str. 33, Main building, Az 1141

Dissertation is accessible at the Baku State University Library.

Electronic version of the abstract is available on the official website of the Baku State University.

Abstract was sent to the required addresses on 22 April 2025.

Signed for print: 04.04.2025
Paper format: A5 (60x90 1/16)
Volume: 36564
Number of hard copies: 20